IOP Publishing Smart Materials and Structures
Smart Mater. Struct. **29** (2020) 105007 (13pp) https://doi.org/10.1088/1361-665X/ab9e07

Shunted magnetostrictive devices in vibration control

Zhangxian Deng[1], Justin J Scheidler[2], Vivake M Asnani[2] and Marcelo J Dapino[3]

[1] Department of Mechanical and Biomedical Engineering, Boise State University, Boise, ID, 83706 United States of America
[2] Rotating and Drive Systems Branch, Materials and Structures Division, NASA Glenn Research Center, Cleveland, OH, United States of America, 44135
[3] Smart Vehicle Concepts Center, Department of Mechanical and Aerospace Engineering, The Ohio State University, Columbus, OH, 43210, United States of America

E-mail: zhangxiandeng@boisestate.edu

Received 10 March 2020, revised 12 May 2020
Accepted for publication 18 June 2020
Published 25 August 2020

Abstract

Structural vibrations in rotating machinery may lead to imprecise motion control, excessive noise, or even structural damage. Magnetostrictive materials can dissipate unwanted vibrations via hysteresis, eddy currents, and joule heating while exhibiting an electrically-tunable elastic modulus. Harnessing this feature, this article presents a shunted magnetostrictive device that includes an iron-gallium (Galfenol) rod, a permanent magnet array, a flux return path, and shunt circuits. The stiffness tunability and damping of this passive device are measured under a 750 Hz sinusoidal axial compression for resistive, capacitive, and inductive shunt circuits. The effect of eddy currents stiffness and damping is investigated for the first time by comparing results from laminated and solid Galfenol rods. Solid Galfenol produces larger eddy current-based damping, while laminated Galfenol enables larger stiffness variation and total damping. This device demonstrates a power density of 19.83 mW cm^{-3} for vibration energy harvesting. The frequency-dependent behavior of the shunted device is tested from 5 Hz to 1 kHz for selected electrical loads.

Keywords: Galfenol, shunt damping, stiffness tuning, energy harvesting

(Some figures may appear in colour only in the online journal)

1. Introduction

Excessive vibrations in power transmission systems can cause negative effects, including detrimental noise, structure damage, or degraded motion control accuracy. The vibration response can be attenuated by tuning the system's natural frequency or introducing structural damping. Stiffness tuning has been achieved passively by varying the pre-stress in a buckled system [1]. However, continuous adjustment of pre-stress in real-time is inconvenient. Recent studies have implemented piezoelectric or electromagnetic transducers for active- or semi-active stiffness tuning [2, 3] in which external power sources are required to drive the transducers. Davis and Lesieutre [4] have experimentally validated a passive stiffness tuning device based on the Young's modulus change in piezo ceramics. But its application in harsh loading conditions is hampered by the brittless of piezo ceramics. Frequency tuning requires knowledge of the forcing frequency and targets few selected modes. Structural damping, however, can mitigate vibrations over a broad operating range. Global reductions to the aforementioned negative effects can be realized by attenuating the vibration at or near its source. Traditional methods based on fluids or viscoelastic materials introduce significant mass to the system and exhibit relatively low stiffness. If these materials are used in or near power transmission subsystems that require precise positioning (e.g. gearboxes, bearings, and antenna pointing drives), their low stiffness can compromise the alignment of components, which usually causes vibration to increase in spite of the added damping. Hence, controlling vibration at or near its source in power transmission systems requires vibration control devices that maintain the high stiffness of the system.

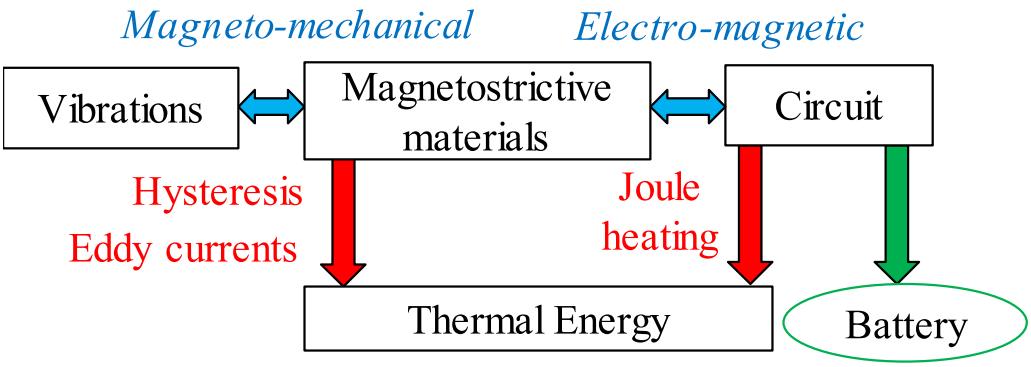

Figure 1. Energy dissipation mechanisms in a shunted magnetostrictive device.

Magnetostrictive material such as terbium-iron-dysprosium alloys (Terfenol-D) and iron-gallium alloys (Galfenol) can provide natural frequency tuning and enhance structural damping while maintaining high stiffness in a solid-state package. Shunted magnetostrictive transducers, consisting of magnetostrictive materials, permanent magnets, and shunted circuits, have been developed as tunable springs and dampers in previous studies [5, 6]. The stiffness tuning of magnetostrictive materials originates from the stress- and magnetic-field-dependent Young's modulus, also known as the ΔE effect. Magnetostrictive materials simultaneously experience elastic deformation S_e and magnetic-field-induced deformation λ under uniaxial loading. Magnetic-field-induced deformation, also known as magnetostriction, is caused by magnetic domain rotation and is a function of applied stress T and magnetic field H. As a result, the Young's modulus E of magnetostrictive materials is

$$E(H,T) = \frac{T}{S_e + \lambda(H,T)}. \quad (1)$$

The ΔE effect has been experimentally characterized in the literature [7–10]. The permanent magnets in shunted magnetostrictive devices provide a constant magnetic flux bias. Due to the electro-magnetic coupling, the electric shunt connected to the magnetic circuit changes the magnetic flux distribution across the magnetostrictive materials and, therefore, enables passive tuning of the device's stiffness.

The energy transformation, as presented in figure 1, allows for tunable damping in shunted magnetostrictive devices. Due to the unique magneto-mechanical coupling in magnetostrictive materials, mechanical energy is first converted to magnetic energy, which is dissipated via hysteresis and eddy currents. Following Faraday's law, magnetic energy variation introduces an electrical potential across the shunted circuit, which induces additional energy dissipation through Joule heating. The hysteresis loss of magnetostrictive materials has been measured from monolithic elements [11–15], micro-scale thin films [16], and particulate composites [17]. Eddy current loss of magnetostrictive materials has been analyzed numerically [18, 19] and characterized experimentally [20, 21]. Recent studies demonstrated that the damping effect is related to the electrical impedance of the shunt circuit [5, 22, 23]. By replacing the shunted circuit with energy storage units, vibratory energy can be scavenged and utilized to power controllers or sensors [24]. Hence, shunted magnetostrictive devices can be self-sustained and multifunctional.

Due to its brittleness, Terfenol-D exhibits low reliability in shunted magnetostrictive devices [25]. Galfenol is mechanically-robust and can be conventionally machined into complex geometries. This study develops a shunted magnetostrictive device using either solid or laminated polycrystalline, <100>-oriented, highly-textured $Fe_{81.6}Ga_{18.4}$ rods, and characterizes the device performance under axial mechanical excitation. This solid-state device can be installed at the vibration source to attenuate structural vibrations before they propagate throughout the system, thereby providing global vibration and noise reduction. The stiffness and damping tuning is contactless through electro-magnetic field interaction.

A shunted magnetostrictive device based on laminated Galfenol has been built and tested to experimentally validate a model [5]. However, the device underperformed due to the lack of magnetic flux path design. Further, only a limited set of data was presented; the influence of eddy currents and inductive shunt circuits has not been measured. To improve shunted magnetostrictive devices, this study re-designs the magnetic flux path, presents a complete characterization of the device's impedance- and frequency-dependent responses for resistive, capacitive, and inductive shunts, and investigates the effect of eddy currents. Additional measurements are obtained to separate the mechanical energy dissipated through the device into its components: the energy loss in the magnetostrictive material, the coil, and the shunt circuit. This separation enables a deeper understanding of the device and a direct comparison of the measured trends to an existing model that neglects losses in the material. Moreover, this paper presents measurements of the electrical energy that can be harvested from the device.

Device configuration and experimental setup are explained in section 2. Performance metrics describing the damping effect, the stiffness variation, and the energy conversion capability are summarized in section 3. In section 4, the performance of the shunted magnetostrictive device is characterized. Measurements are made under various resistive, capacitive, and inductive loads at 750 Hz. The frequency-dependent behavior at selected load impedance is then measured up to 1 kHz. Finally, the influence of mechanically-induced eddy

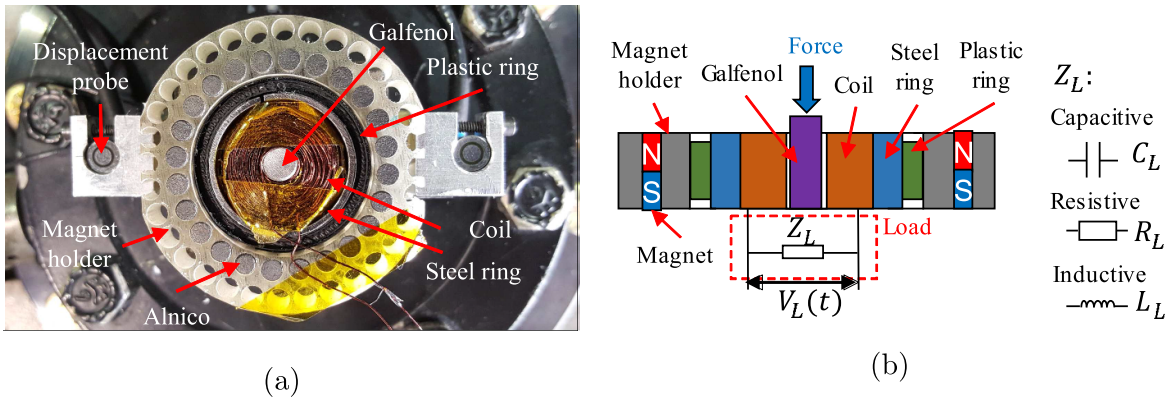

Figure 2. (a) Physical assembly and (b) schematic of the shunted magnetostrictive device based on Galfenol.

currents is studied by comparing the measurements based on solid and laminated Galfenol rods.

2. Experimental setup

Figure 2 shows the shunted magnetostrictive device used in this study. Details of the device configuration, equivalent electric circuits, and preliminary characterization results in quasi-static regime have been presented in reference [26]. To explore the effect of eddy currents, solid and laminated <100>-oriented, highly-textured, polycrystalline $Fe_{81.6}Ga_{18.4}$ rods are tested. Material properties of the Galfenol alloys used in this study have been presented in references [9] and [21]. Each rod has a radius of 3 mm and a length of 10 mm. A laminated rod composed of 0.84 mm thick laminates that were cut along the rod's axial direction can effectively mitigate eddy current loss up to 1 kHz [21]. Thinner laminates could better mitigate eddy currents, but also reduce the volume fraction of Galfenol for a given rod diameter. Here, the laminated rod is composed of 6 sections (less than 0.5 mm per laminate) that are bonded together with epoxy (EI-Cast 760 epoxy and 215 hardener) [21]. The electrically-insulating adhesive layer is 45.7-50.8 microns thick. A 9.5 mm long, 500-turn pickup coil made of AWG 30 copper wire surrounds the rod to convert the stress-induced magnetic flux density variation to an electrical voltage. The coil resistance R_c is 6.89 Ω, whereas its inductance L_c varies due to the stress- and field-dependent magnetic permeability of Galfenol.

A 3D-printed plastic ring is utilized to hold 24 Alnico (grade 8) permanent magnets at an even spacing around the rod. Each magnet is magnetized along the axial direction (see figure 2(b)) and has a nominal remanent flux density of 0.36 T and is 3.175 mm in diameter and 9.525 mm in length. The uniformity of the magnet-produced flux in the magnetostrictive rod is confirmed via finite element modeling in a commercial multiphysics software. Another 3D-printed plastic ring is placed between the magnetic holder and the steel ring to ensure concentric alignment. Compared to the device in reference [5], this study adds a magnetic flux path, or a magnetically-conductive AISI 1006 low carbon steel ring. The magnetic permeability of Galfenol is much higher than that of the coil and ambient air. Without the low carbon steel ring, the Galfenol rod is always the preferred path for magnetic flux. Therefore, the coil sees a smaller variation in magnetic flux density and, thus, a smaller induced electrical response. The low carbon steel ring, which has a similar magnetic reluctance to the Galfenol rod, offers another preferred magnetic flux path. This has the effect of increasing the device's magnetoelectric sensitivity, because magnetic flux redistributes into the steel ring (and out of the coil), even for smaller changes in the rod's magnetic permeability. Previous studies have validated that such a low carbon steel ring could enhance the performance of shunted magnetostrictive devices [19, 26]. The inner and outer diameter of the steel ring are 19.05 mm and 21.05 mm, respectively. A 1 mm wide gap is cut into the steel ring along its axis to mitigate its eddy current losses. To maximize the magneto-mechanical coupling in the device, the dimensions of both the steel ring and the permanent magnet configuration are selected based on numerical simulation and experimental characterization [26, 27].

As depicted in figure 3, a dynamic load frame operating in force control mode supplies axial forces at frequencies up to 1 kHz. A spherical joint is used in the load path to improve the uniformity of contact with the rod. The attached electrical loads include resistive, capacitive, and inductive components, as shown in figure 2(b). The actual electrical impedance Z_L connected to the pickup coil is calibrated using a precision LCR meter. Compared to a previous experimental setup designed for a Terfenol-D-based shunted device [6], this study considers the magnetic flux leakage as an additional variable that needs to be controlled. An iron powder core (Fe-Si, 1.67 T saturation, relative magnetic permeability of 60) is placed on each end of the shunted magnetostrictive device to form a closed magnetic flux path to prevent eddy currents in the surrounding components (e.g. top target, probe holder).

The calculation of the device's stiffness and loss factor requires accurate measurement of force and deformation. A high stiffness, fatigue-rated load cell with a range setting of ± 2500 N is utilized to measure both the static and dynamic force components. However, the load cell only measures the mechanical force applied by the load frame, but not the magnetic force due to the attraction between the permanent magnets and iron powder plates. The magnetic force measured

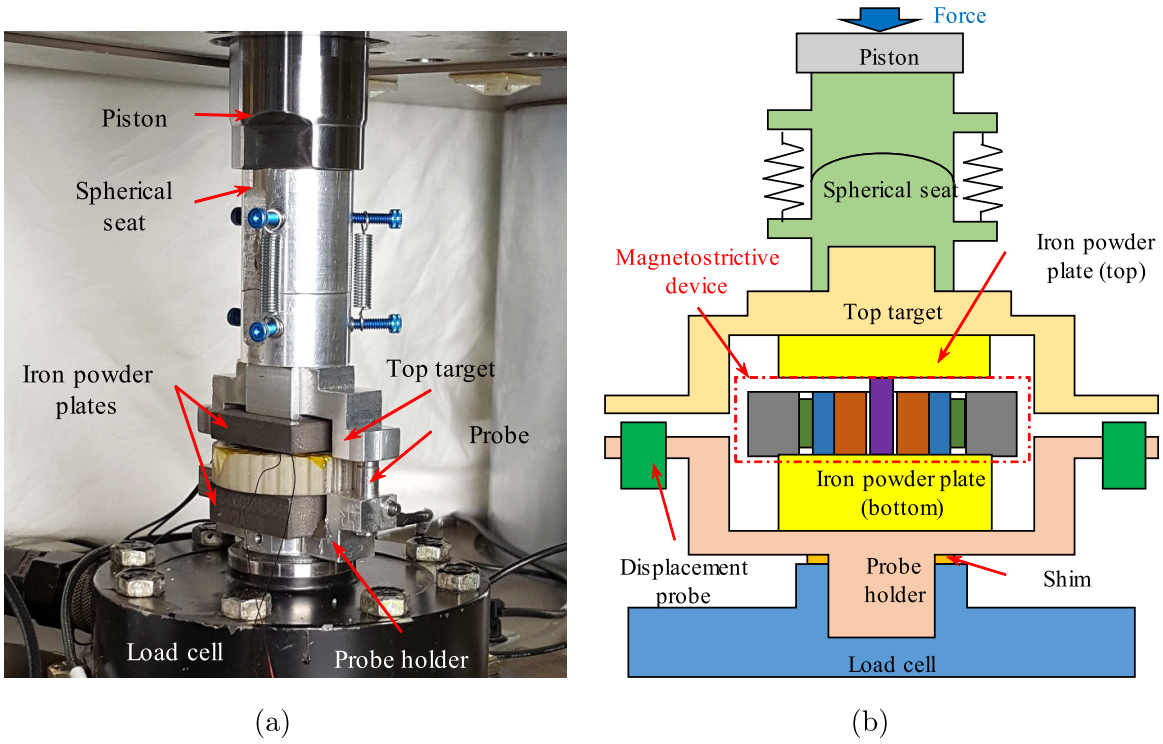

Figure 3. (a) Physical assembly and (b) schematic of the test setup for the shunted magnetostrictive device.

from the device containing a solid and laminated Galfenol rod are 14.19 N and 13.97 N, respectively. The magnetic force is added to the load cell measurement following reference [26]. Any mass in between the rod and load cell cause errors in the force measurement due to inertial force [20]. The error in the dynamic force due to inertial forces is less than 0.6% at 1 kHz. The deformation of the Galfenol rod is measured by a pair of precision capacitive displacement probes, which are held by a U-shaped aluminum part. Each displacement probe provides a range of ± 100 microns with accuracy of better than 0.1%. The average power and power density require precise measurement of voltage across the pickup coil V_L. The influence of the data acquisition system, filters, and connection cables on the voltage measurement has been calibrated and compensated numerically in data post-processing. Finite element simulation in a commercial multiphysics software confirms that the first vibration mode of the physical assembly depicted in figure 3(b) occurs at 4093 Hz, which is much higher than the testing frequencies.

3. Performance metrics

In this study, the vibration force has a frequency of 750 Hz, which is the fundamental gear mesh frequency of a particular helicopter gearbox. The force amplitude is similar to the values used for previous shunted piezoelectric devices to permit a direct comparison [6]. The research objective is to maximize the shunted magnetostrictive device's stiffness variation and energy dissipation capacity under the given vibration source (*i.e.,* its potential for controlling vibration at the source in power transmission systems).

The stiffness of the magnetostrictive device is treated in the same manner as an elastomeric material. Following the Fast Fourier Transform (FFT) method in ASTM D5992-96(2011) [28], the device's stiffness K^* is a complex valued stiffness calculated as

$$K^* = \frac{F^*}{S^*} = K(1 + j\eta_0), \tag{2}$$

where K is the lossless stiffness, η_0 is the total loss factor of the system, $j = \sqrt{-1}$, F^* and S^* are the fundamental harmonics (at excitation frequency f_0) in force and displacement, respectively. Values of K and η_0 are directly extracted from the force-displacement measurements. The value of K has a range from $K_{\min}$ to $K_{\max}$. To quantify the stiffness tunability of the shunted magnetostrictive device, a normalized stiffness variation $\bar{K}$, which is a function of Z_L and f_0, is defined as

$$\bar{K} = \frac{K_{\max} - K_{\min}}{K_{\max}}. \tag{3}$$

The total loss factor η_0 is a ratio of the total energy dissipated per radian of the vibration cycle to the stored energy (kinetic plus potential) associated with vibration (E_{osc}) [29]. The total loss factor is decomposed into the loss factors due to the rod (material hysteresis and eddy current loss) η_{device}, the electrical shunt η_{shunt}, and the pickup coil η_{coil}, by separating the total energy dissipated into the energy dissipated in the rod, shunt (E_{shunt}), and coil (E_{coil}), respectively. Hence, $\eta_0 = \eta_{device} + \eta_{shunt} + \eta_{coil}$.

The value of η_{shunt} is calculated as [29]

$$\eta_{shunt} = \frac{E_{shunt}}{2\pi E_{osc}}. \tag{4}$$

Here, the oscillation energy is

$$E_{osc} = \frac{1}{2}K|S^*|^2. \tag{5}$$

The energy dissipated in the electrical circuit E_{shunt} is [6]

$$E_{shunt} = \frac{1}{2f_0}\left|\frac{V_L^*}{Z_L^*}\right|^2 \mathrm{Re}\left(Z_L^*\right), \tag{6}$$

where V_L^* is the fundamental harmonic of $V_L(t)$ at f_0. For a coil resistance R_c, the energy dissipated in the coil is

$$E_{coil} = \frac{1}{2f_0}\left|\frac{V_L^*}{Z_L^*}\right|^2 R_c. \tag{7}$$

Following the definition of loss factor, the value of η_{coil} is

$$\eta_{coil} = \frac{E_{coil}}{2\pi E_{osc}}. \tag{8}$$

The value of η_{device} is thus calculated as

$$\eta_{device} = \eta_0 - \eta_{coil} - \eta_{shunt}. \tag{9}$$

The electrical energy dissipated by the resistive load R_L is approximately equal to the useful electrical energy that can be scavenged. Hence, the energy harvesting capability, which is described by the average power output $\bar{P}$, is characterized as [24]

$$\bar{P} = \frac{1}{2}\left|\frac{V_L^*}{R_L}\right|^2 R_L. \tag{10}$$

To eliminate the influence of the device's volume, an average power density $\bar{D}$ is defined as [24]

$$\bar{D} = \frac{\bar{P}}{V_G}, \tag{11}$$

where V_G is the volume of the Galfenol rod.

4. Experimental results

Scheidler and Asnani [5] have theoretically proved that the normalized stiffness variation $\bar{K}$ and loss factor η_0 of shunted magnetostrictive devices are simultaneously maximized when maximizing the coupling factor, which is determined by the interplay of magnetic field bias H_0 and mechanical compression bias F_0. For a shunted magnetostrictive device excited by a given dynamic force, the optimal values of H_0 and F_0 will maximize the open circuit voltage across the coil. The value of H_0 is fixed and relies on the permanent magnet configuration, which has been explained in section 2. A constant force F_0 is applied to the shunted device on top of a 750 Hz and 73.51 N amplitude sinusoidal compression, The value of F_0 is gradually increased until the resulting open circuit voltage peaks. Following this approach, the bias compression F_0 for the laminated and solid Galfenol rods is determined to be 746 N and 604 N, respectively. The non-magnetically-conductive adhesive layers in the laminated sample reduce its effective magnetic permeability and result in increased H_0. Hence, a larger F_0 is required to balance the larger H_0 for the laminated Galfenol sample.

This study first investigates the stiffness variation and damping of the shunted magnetostrictive device based on laminated Galfenol and using resistive, capacitive, or inductive shunts. A 750 Hz sinusoidal compression is selected as the mechanical excitation. For selected resistive and capacitive shunts, the rate-dependent performance of the shunted device is investigated between 5 Hz and 1 kHz. Due to the nonlinearity in material properties and control inaccuracy, the actual applied force consists of the fundamental component as well as unavoidable higher harmonics. The unwanted 2nd harmonics have a magnitude of $\leq 4.2\%$ relative to the desired stress sinusoid within the aforementioned frequency range. The unwanted 3rd harmonics typically have a magnitude of $\leq 4.9\%$ relative to the desired stress sinusoid except for a narrow frequency range from 372 Hz to 398 Hz, where the 3rd harmonics have a magnitude of $\leq 13.5\%$. To quantify the influence of eddy currents, the tests are repeated for the shunted device based on solid Galfenol. A test without the electrical shunt is also completed to quantify the damping introduced by the eddy current loss alone.

4.1. Laminated Galfenol - Impedance sweep

4.1.1. Resistive sweep. A 750 Hz, 73.51 N amplitude sinusoidal force F_d, together with an DC force $F_0 = 746$ N, is applied on the laminated Galfenol rod. The corresponding loss factor η_0 and stiffness K are measured under different resistive loads R_L. Figure 4(a) shows the bell-shaped loss factor η_0 as R_L increases from short circuit to open circuit. This trend mirrors the trend predicted by the quasi-linear model in reference [5]. The loss factor η_0 reaches the maximum value of 0.061 when $R_L = 138.2\ \Omega$. When the pickup coil is shorted or open, the energy loss on the shunt circuit is negligible and $\eta_0 = \eta_{device} = 0.009$. Due to the negligible eddy currents in the laminated Galfenol rod, η_{device} is mainly introduced by material hysteresis. The electrical shunt accounts for more of the loss factor than the pickup coil, except for resistance less than about 8 Ω.

Figure 4(b) shows that the stiffness K of the laminated Galfenol rod decreases monotonically from 74.9 N/μm to 66.7 N/μm as R_L increases, which corresponds to a $\bar{K}$ of 11.0%. This observation matches previous quasi-static measurements [30]. According to the Stoner-Wohlfarth approximation, bulk magnetostrictive materials are composed of non-interacting magnetic domains. An external magnetic field rotates the magnetic domains, causes macroscopic deformation, or magnetostriction, and varies the material's stiffness. In a shunted magnetostrictive device, the induced current in the pickup coil generates an additional magnetic field H_d on top of the bias field that is provided by permanent magnets. Under resistive loading, H_d prevents magnetic domain rotation, reduces magnetostriction, and correspondingly increases

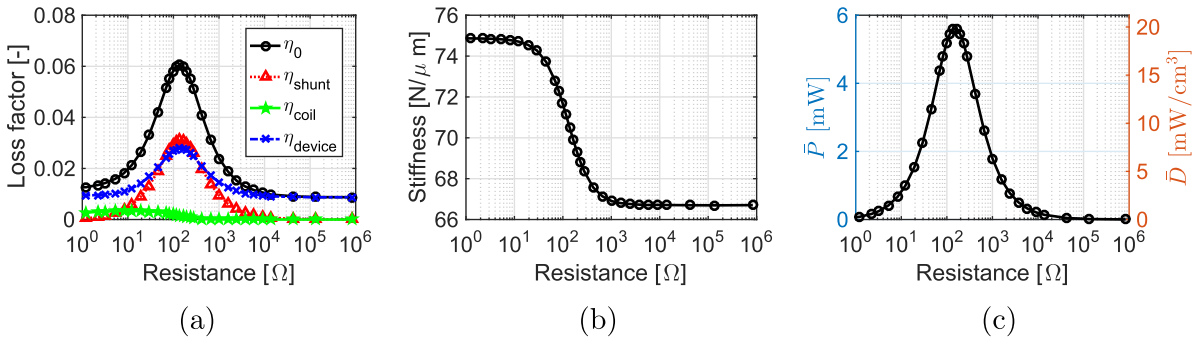

Figure 4. (a) Loss factor, (b) stiffness, and (c) energy harvesting capacity measured from the shunted device based on the laminated Galfenol and resistive load.

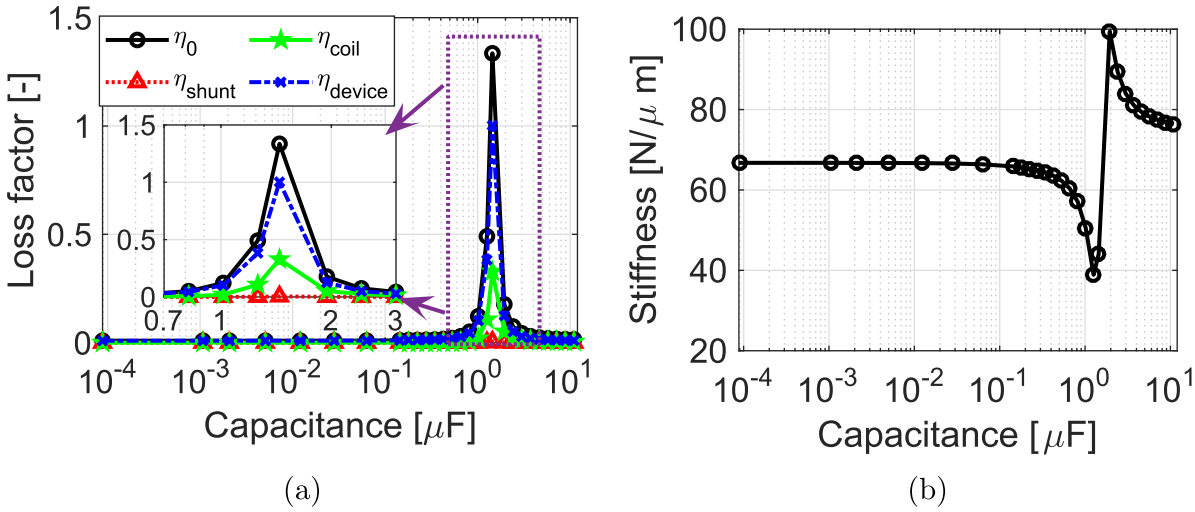

Figure 5. (a) Loss factor and (b) stiffness from the shunted device based on the laminated Galfenol and capacitive load.

the stiffness of the Galfenol rod. When the coil is shorted, the induced current and H_d are maximized and accordingly the stiffness. This trend also mirrors that was predicted in reference [5].

The maximum $\bar{P}$ and $\bar{D}$ are 5.61 mW and 19.83 mW cm^{-3}, respectively, when $R_L = 138.2\ \Omega$. The amount of electrical energy scavenged from the system is large enough to power micro-controllers and sensors. Hence, future dampers or isolators based on a shunted magnetostrictive device can be simultaneously adaptive and self-sustainable. However, the energy harvesting capability is lower than that of similar shunted piezoelectric devices, since the coil dissipates considerable amount of electrical energy.

4.1.2. Capacitive sweep. Magneto-electric coupling can be further amplified in the shunt circuit by complementing the coil's inductance with a capacitive shunt to create a resonant response. The same sinusoidal force F_d together with static force F_0 are applied on the laminated Galfenol rod for different capacitive loads C_L. A maximum loss factor $\eta_0 = 1.34$ is obtained when $C_L = 1.44\ \mu$F and an electrical resonance is created, as shown in figure 5(a). The maximum η_{shunt} and η_{device}, which are also observed at $C_L = 1.44\ \mu$F, are 0.33 and 1.01, respectively. Figure 5(b) shows a large discontinuity in stiffness around the resonance. As C_L increases from 1.26 μF to 1.94 μF, the stiffness K increases from 38.9 N/μm to 99.4 N/μm corresponding to a $\bar{K}$ value of 60.9%. The stiffness drops below the open circuit value and increases above the short circuit value around the electrical resonance.

4.1.3. Inductive. The shunted magnetostrictive device is tested for different inductive loadings under the same sinusoidal force F_d and static force F_0. As shown in figure 6(a), the inherent resistance of the inductor coils create small but appreciable loss factors, which needs to be considered for improving the accuracy of the quasi-linear model [5]. When L_L is smaller than 1 mH, the measurement is similar to the shorted condition shown in figure 4. Due to energy loss on R_c, the loss factor $\eta_{shunt} = 0.004$ when $L_L = 0.1$ mH. When L_L is large (> 0.1 H), the electrical impedance is relatively high and the system response is similar to the open-circuit results shown in figure 4. For instance, the loss factor at $L_L = 11.11$ H is 0.009, which is primarily due to the material's hysteresis. The stiffness variation is also similar to that of the resistive shunt. The stiffness K decreases from 75.2 N/μm to 67.0 N/μm when L_L increases from 0.1 mH to 11.11 H. Compared to the results of the resistive load sweep, varying the inductive load provides

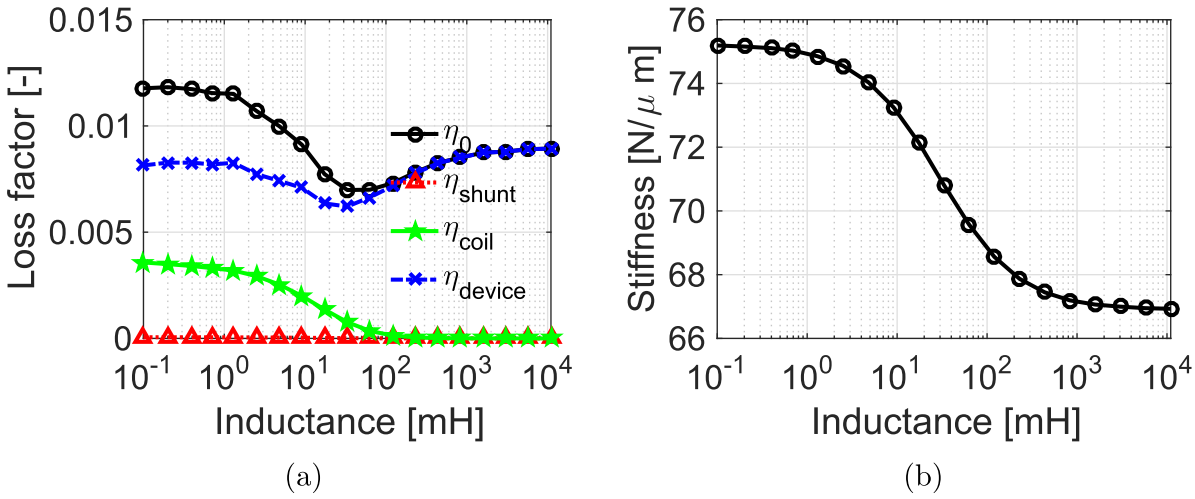

Figure 6. (a) Loss factor and (b) stiffness from the shunted device based on the laminated Galfenol rod and inductive load.

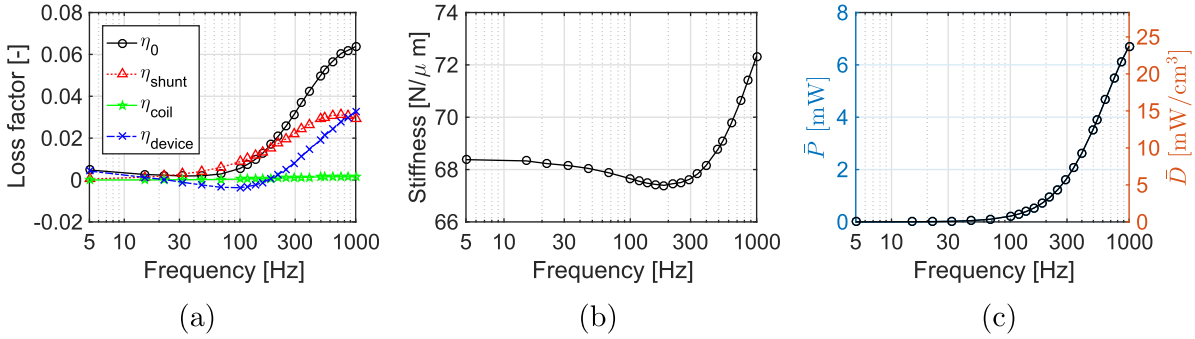

Figure 7. (a) Loss factor, (b) stiffness, and (c) energy harvesting capacity measured from the shunted device based on laminated Galfenol for an excitation frequency between 5 Hz and 1 kHz ($R_L = 138.2\ \Omega$).

a similar $\bar{K}$ value without significantly changing the system's damping effect.

4.2. Laminated Galfenol - Frequency sweep

4.2.1. Resistive. A 78.51 N amplitude sinusoidal force F_d' superimposed on the selected bias force $F_0 = 746$ N is applied on the laminated Galfenol rod. The resistive load connected to the pickup coil is $R_L = 138.2\ \Omega$. The excitation frequency f_0 of F_d' changes from 5 Hz to 1000 Hz. The rate-dependent loss factor and stiffness are presented in figure 7.

The material hysteresis loss per vibration cycle, which is due to pinning site loss, is frequency independent [21, 32]. The value of η_0 increases from 0.004 to 0.064 as f_0 varies from 5 Hz to 1000 Hz. The value of η_{shunt} initially increases with respect to the excitation frequency. Eddy currents induce magnetic field diffusion in a magnetostrictive rod, thereby reducing magnetic flux density variation and, thus, the voltage across the shunt [18, 31]. The loss factor η_{shunt} starts to decline around 750 Hz, since the resistant shunt is tuned to peak at 750 Hz. A slightly negative η_{device} is observed between 38 Hz and 195 Hz. This measurement error is likely due to a small inaccuracy in the phase calibration procedure for the displacement probes, leading to an over-compensation of the phase lag introduced by the sensor and its conditioning electronics over this frequency range. Figure 7(b) shows that the stiffness of the laminated Galfenol rod slightly drops around 200 Hz and then increases. The initial drop in stiffness is still under investigation. The stiffness increment after 200 Hz is induced by the increasing current in the shunt circuit and an increase in eddy currents. The large induced current through the coil generates an additional magnetic field H_d which prevents domain rotation, thus increasing system stiffness. The loss factor η_{device} due to material hysteresis and eddy currents is

$$\eta_{device} = \frac{E_{device}}{2\pi E_{osc}} = \frac{E_{device} K}{\pi |F^*|^2}. \tag{12}$$

For the laminated Galfenol rod, E_{device} mainly includes the material's hysteresis loss, which is independent of f_0. The force amplitude $|F^*|$ is held constant. Hence, the trend of η_{device} follows the trend of K, as shown in figure 7.

Figure 7(c) presents the average power and power density available from the laminated Galfenol rod for different excitation frequencies. As f_0 increases from 5 Hz to 1 kHz, $\bar{P}$ monotonically increases from 0.58 μW to 6.85 mW while $\bar{D}$ monotonically increases from 2.04 μW/cm^3 to 6.85 mW cm^{-3}.

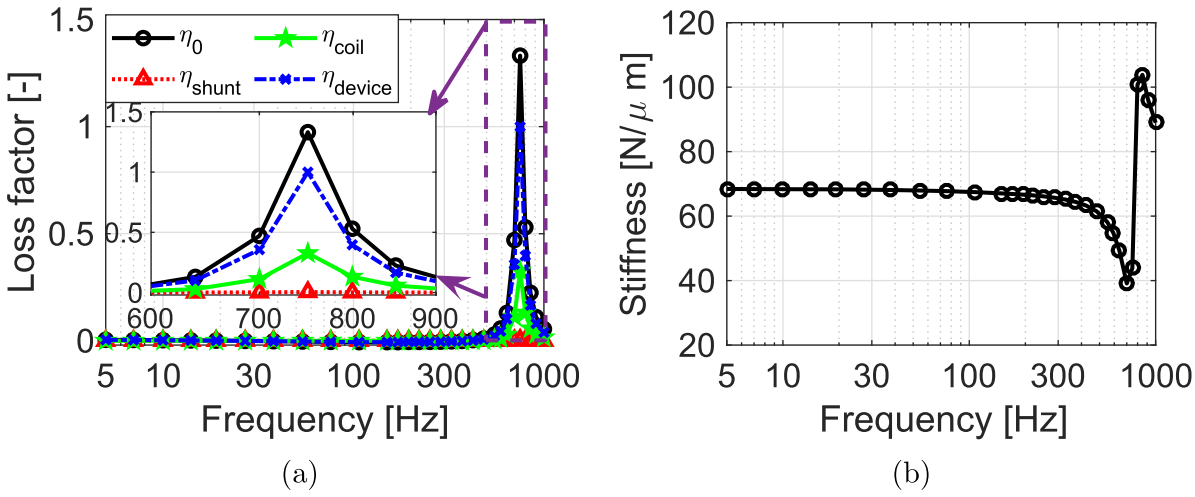

Figure 8. (a) Loss factor and (b) stiffness from the shunted device based on laminated Galfenol for an excitation frequency between 5 Hz and 1 kHz ($C_L = 1.44$ μF).

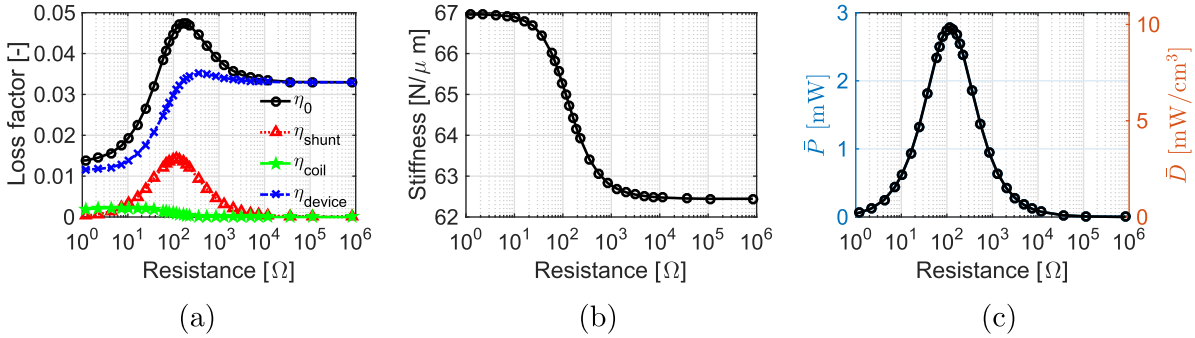

Figure 9. (a) Loss factor, (b) stiffness, and (c) energy harvesting capacity measured from the shunted device based on the solid Galfenol and resistive load.

4.2.2. Capacitive. The mechanical loading is the same as for resistive frequency sweep while the capacitive load attached to the pick coil is $C_L = 1.44$ μF, which maximizes the loss factor in the capacitive sweep at 750 Hz. Figure 8(a) shows that the loss factor exceeds one around the electrical resonance, which is set at 750 Hz in this study. Control algorithms that automatically tune the capacitive load and track the excitation frequency f_0 can be developed in the future to expand the frequency bandwidth of a resonantly-shunted magnetostrictive device. The stiffness of the laminated Galfenol rod varies from 39.1 N/μm to 103.8 N/μm, or by 62.3%, when the excitation frequency f_0 increases from 700 Hz to 850 Hz. A resonant shunt can provide a significant amount of narrowband damping at the device level, but it is accompanied by a large change in stiffness.

4.3. Solid Galfenol - Impedance sweep

4.3.1. Resistive sweep. A 750 Hz, 73.51 N amplitude sinusoidal force F_d along the selected bias force $F_0 = 604$ N is applied on the solid Galfenol sample. The corresponding loss factor and stiffness measured under different resistive loads R_L are presented in figure 9.

Compared to the loss factor measurements of the device based on laminated Galfenol shown in figure 4(a), the trend of η_{device} is different due to the interplay of the induced current in the pickup coil and the eddy current in the solid rod. The value of η_{device} consists of material hysteresis and eddy current loss in the solid Galfenol rod. When the pickup coil is shorted, the induced current is maximized, and it creates an additional magnetic field that counteracts the magnetic bias and eventually suppresses the eddy currents. Hence, η_{device} is dominated by the material's hysteresis and reaches the minimum of 0.012, which, as expected, is very similar to the 0.009 minimum observed for the laminated rod. As the load impedance increases, the induced current in the coil reduces and thus the influence of eddy current becomes significant. When the pickup coil is open, the eddy current loss is maximized. According to figure 4(a), the material hysteresis peaks when the load impedance matches R_{opt} in reference [5]. Due to the combined effect of material hysteresis and eddy current loss, η_{device} reaches a maximum value of 0.035 when $R_L = 354.2$ Ω. The trend of η_{shunt} is similar to the measurement from the device based on laminated Galfenol. The peak value of η_{shunt} (0.015 at $R_L = 97.2$ Ω) is less than half of that observed from the laminated rod, since the eddy currents create magnetic field diffusion that reduces the magneto-mechanical coupling

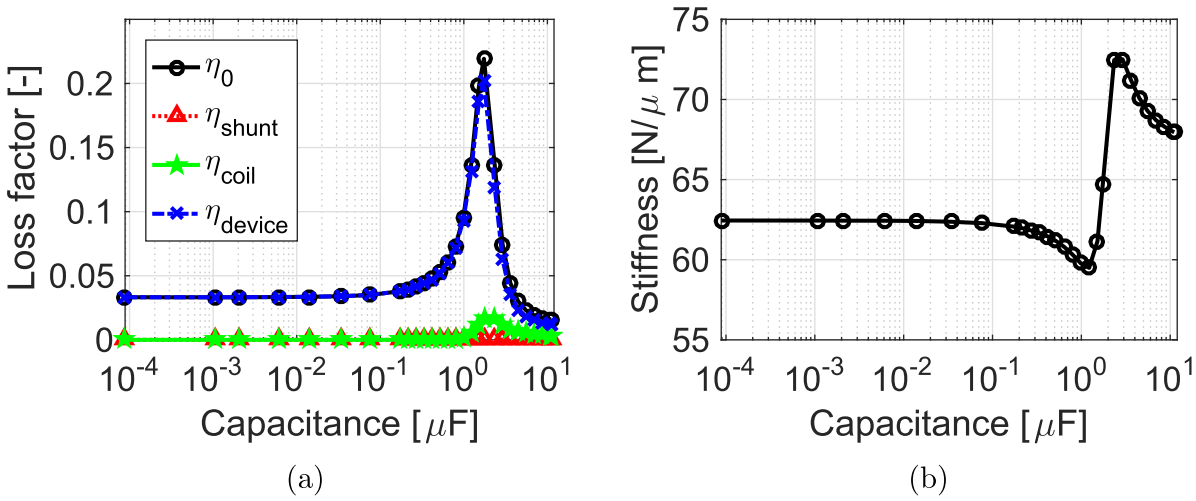

Figure 10. (a) Loss factor and (b) stiffness from the shunted device based on solid Galfenol and capacitive load.

in the Galfenol, and thus the overall magneto-electric coupling. The combined η_{device} and η_{shunt} provide a maximum loss factor $\eta_0 = 0.048$ when $R_L = 162.2\ \Omega$, which is only 79% of that from the laminated device. Overall, the eddy currents in solid Galfenol are detrimental to system damping.

Figure 9(b) shows that the stiffness of the shunted device based on solid Galfenol decreases monotonically from 67.0 N/μm to 62.5 N/μm, when the shunt resistance varies from 0.22 Ω (shorted) to 0.83 MΩ (open circuit). This corresponds to a relative stiffness variation of $\bar{K} = 6.7\%$. Compared with the device based on laminated Galfenol (figure 4(b)), the reduction of $\bar{K}$ is due to the magnetic field diffusion in the solid Galfenol device that prevents magnetic domain rotation and, thus, reduces magnetostriction [18, 31]. The shunted device based on solid Galfenol exhibits a relatively low stiffness even without the laminated Galfenol rod's soft adhesive layers. This is caused by the stress-dependent Young's modulus of Galfenol and the difference in selected bias force F_0 between the two tests [9].

As shown in figure 9(c), the maximum value of the average power $\bar{P}$ and average power density $\bar{D}$ are 2.78 mW and 9.83 mW cm^{-3}, respectively, when $R_L = 115.2\ \Omega$. Due to the magnetic field diffusion induced by eddy currents, the power generated from the shunted magnetostrictive device based on solid Galfenol is 50.5% of that based on laminated Galfenol.

4.3.2. Capacitive sweep. As with the shunted device based on laminated Galfenol, the loss factor can be significantly improved by attaching a capacitor to the pickup coil to maximize the magneto-electric coupling over a narrow frequency bandwidth, as shown in figure 10(a). The same dynamic force F_d and the selected bias force F_0 are applied on the shunted device based on solid Galfenol. The maximum η_0 and η_{shunt} are 0.219 and 0.017, respectively, when $C_L = 1.44\ \mu$F. The bounds of the η_{device} response (0.033 at minimal capacitance and 0.012 at maximal capacitance) are respectively equal to the open and short circuit η_{device} from the resistance sweep test. Figure 10(b) shows that the stiffness increases from 59.5 N/μm to 72.5 N/μm as C_L increases from 1.22 μF to 2.91 μF. This corresponds to a $\bar{K}$ of 17.9%. Compared to the results from the shunted device based on laminated Galfenol, the damping effect and stiffness variation are much smaller due to increased eddy currents in the device based on solid Galfenol.

4.3.3. Inductive sweep. Figure 11 presents the loss factor and stiffness measurement for various inductive loads under the same dynamic and static force. When $L_L = 0.1$ mH and the electrical impedance is low, the loss factor $\eta_0 = 0.014$ is similar to the shorted condition. When $L_L = 11.11$ H and the electrical impedance is high, the loss factor $\eta_0 = 0.033$ is the same as the open circuit value observed in the resistive sweep. Due to the additional energy loss introduced by eddy currents, the loss factor variation is larger than that observed from the shunted device based on laminated Galfenol, shown in figure 6(a). The stiffness K decreases from 67.1 N/μm to 62.6 N/μm monotonically as L_L changes from 0.1 mH to 11.11 H. The normalized stiffness variation is 6.7%, which equals the value achieved from the resistive sweep, but is much less than the value obtained from the shunted device based on laminated Galfenol.

4.4. Solid Galfenol - Frequency sweep

4.4.1. Resistive. In this test, a sinusoidal force F_d with an amplitude of 73.51 N superimposed on the selected bias force $F_0 = 604$ N is applied on the shunted device based on solid Galfenol. The resistive load that maximizes the loss factor η_0 ($R_L = 115.2\ \Omega$) is connected to the pickup coil. The excitation frequency f_0 varies from 5 Hz to 1000 Hz. The rate-dependent loss factor and stiffness are presented in figure 12.

The value of η_{shunt} initially increases with increasing f_0. As f_0 exceeds a certain value, the eddy currents dominate, thus reducing magneto-mechanical coupling in the pickup coil. Hence, a maximum $\eta_{shunt} = 0.013$ is observed at 541 Hz. According to equation (12), the trend of η_{device} follows the trend of K. The initial drop in K around 200 Hz, which is

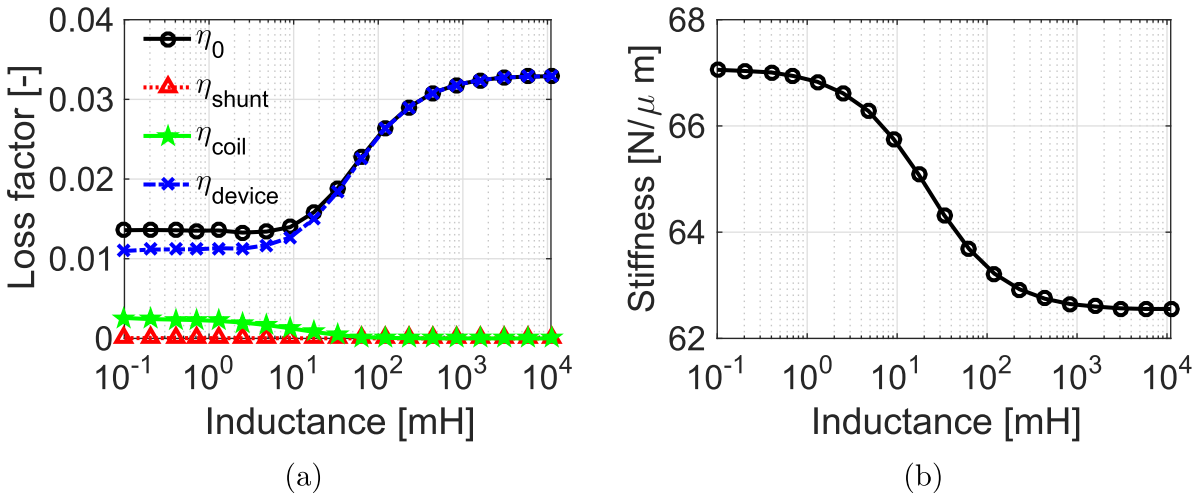

Figure 11. (a) Loss factor and (b) stiffness from the shunted device based on solid Galfenol and inductive load.

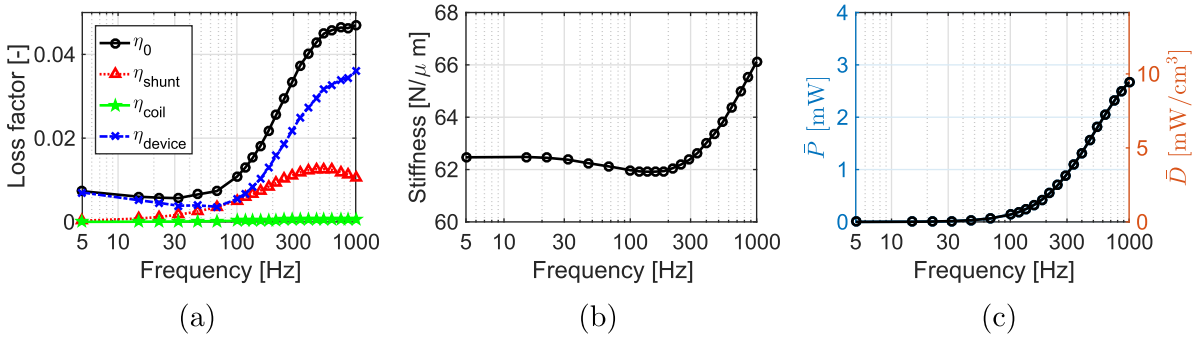

Figure 12. (a) Loss factor, (b) stiffness, and (c) energy harvesting capacity measured from the shunted solid Galfenol for an excitation frequency between 5 Hz and 1 kHz ($R_L = 115.2\ \Omega$).

also observed from the shunted device based on laminated Galfenol, is under investigation. At high frequencies, large induced current in the coil and eddy currents suppress magnetic moment rotation. As a result, the system's stiffness increases above 200 Hz. Compared to the loss factor measurement presented in figure 7(a), the value of η_0 from the shunted device based on solid Galfenol is larger than that from the laminated device below 300 Hz. Beyond 300 Hz, η_0 from the shunted device based on laminated Galfenol is larger. This indicates that the eddy current loss or the laminations are beneficial to create more system damping when there is small to moderate excitation frequency.

The average power and average power density measured from the shunted device based on solid Galfenol are presented in figure 12(c) as a function of excitation frequency f_0. As f_0 is increased from 5 Hz to 1 kHz, $\bar{P}$ increases from 0.38 μW to 2.67 mW and $\bar{D}$ increases from 1.33 μW/cm^3 to 9.45 mW cm^{-3}. The power generated from the shunted device based on solid Galfenol is less than that from laminated Galfenol over the entire frequency range.

4.4.2. Capacitive. The same dynamic force F_d' with a varying frequency f_0 is applied on the solid Galfenol rod when a capacitive load $C_L = 1.74$ μF is attached to the pickup coil. Due to the electrical resonance, a peak of $\eta_0 = 0.219$ is achieved at 750 Hz, as shown in figure 13(a). The value of η_0 drops quickly when f_0 shifts away from resonance. Figure 13(b) shows that stiffness of the solid Galfenol rod varies from 58.3 N/μm to 73.3 N/μm, or by 20.5%, when the excitation frequency f_0 increases from 593 Hz to 945 Hz. The solid Galfenol rod exhibits a relatively small damping effect, as well as stiffness variation around the electrical resonance.

4.5. Solid Galfenol - Eddy current effect

Deng and Dapino [19] have recently designed a Galfenol-based and coil-less damper that takes advantage of stress-induced eddy current loss and material hysteresis alone. This damper concept is tested experimentally in this study by disconnecting the electrical shunt from the coil shown in figure 3(a). A dynamic force with an amplitude of 73.51 N and a variable frequency of f_0 together with two different bias forces is applied to the shunted device based on solid Galfenol. The corresponding loss factors and stiffness are presented in figure 14. When a large compression force $F_0 = 2364$ N is applied, the Galfenol rod is mechanically saturated. In this saturation state, magnetic domains are oriented in the plane that is perpendicular to F_0 and no magneto-mechanical coupling exists. Hence, the loss factor is negligible and the stiffness

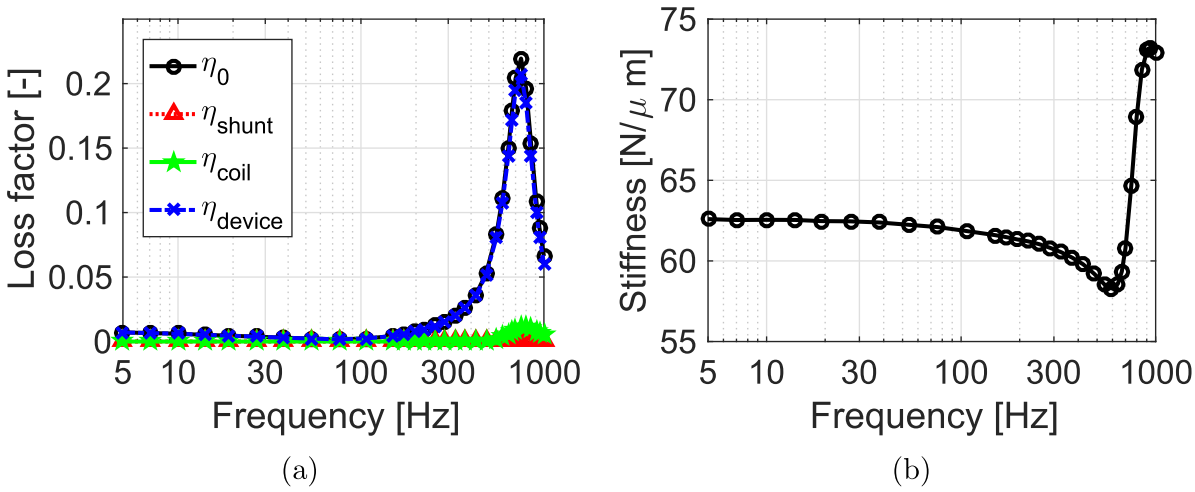

Figure 13. (a) Loss factor and (b) stiffness of the solid Galfenol rod at $C_L = 1.74$ μF, when excitation frequency increases from 5 Hz to 1 kHz.

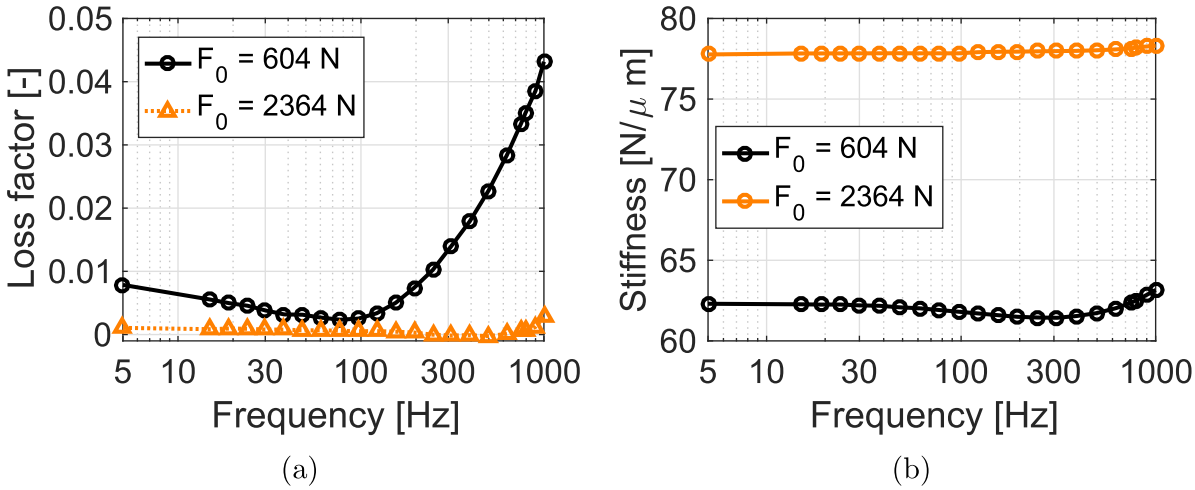

Figure 14. (a) Loss factor and (b) stiffness from the shunted device based on solid Galfenol from an excitation frequency between 5 Hz and 1 kHz (open circuit shunt).

stays at a constant value of about 78 N/μm. The loss factor η_0 gradually drops below 200 Hz and dramatically increases afterwards, when the bias force $F_0 = 604$ N and the solid Galfenol rod operates about its most active bias state. Due to the significant magneto-mechanical coupling, a maximum loss factor of 0.043 is achieved at 1 kHz. However, the initial drop of η_0 before 77 Hz is under investigation. Since $\eta_0 = \eta_{device}$ in this case, the initial drop in η_0 is possibly due to the drop in stiffness below 200 Hz. Utilizing the material hysteresis and stress-induced eddy current loss, magnetostrictive devices of this type can passively dissipate unwanted vibration without the bulky pickup coil and shunt circuit. This type of device can also be adaptive by controlling the bias force on the magnetostrictive elements. However, the reduction in complexity comes at the expense of reduced damping and stiffness tuning range, particularly compared to resonant shunts and if the excitation frequency is below the magnetostrictive material's cut-off frequency for mechanically-induced magnetic diffusion [18].

5. Discussion

The stiffness of the shunted magnetostrictive device is a function of the shunt's electrical impedance, as shown in table 1. The maximum loss factor and the associated frequency bandwidth are presented in table 2. The device presented in this study exhibits much higher loss factors and stiffness variations compared to the one presented in reference [5] due to the enhanced magneto-mechanical coupling enabled by the additional magnetic flux path. The improved performance will facilitate more effective vibration control with no change in the device's form factor and a minimal increase in its mass. Key observations include:

- Resistive load - the loss factor η_0 is maximized when the resistive load matches the optimal resistance in reference [5]; the stiffness K decreases monotonically as the load's resistance increases.

Table 1. Measurement of relative stiffness variation $\bar{K}$.

Z_L	0.22 Ω-0.83 MΩ	1.26 μF-1.94 μF	0.1 mH-11.11 H
$\bar{K}$ (Laminated)	11.0%	60.9%	10.9%
$\bar{K}$ (Solid)	6.7%	17.9%	6.7%

Table 2. Measurement of η_0 and associated frequency bandwidth (BW). (L: laminated; S: solid).

Z_L	η_0 (L)	η_0 (S)	BW (L)	BW (S)
138.2 Ω	0.061	0.048	433-1000 Hz	290-1000 Hz
1.44 μF	1.336	0.219	727-774 Hz	644-851 Hz
33.2 mH	0.012	0.033	n/a	n/a

Table 3. Measurement of $\bar{P}$ and $\bar{D}$.

Material	R_L (Ω)	$\bar{P}$ (mW)	$\bar{D}$ (mW cm^{-3})
Laminated	138.2	5.61	19.83
Solid	115.2	2.78	9.82

- Capacitive load - values of η_0 and $\bar{K}$ can be significantly improved by attaching a capacitor to the pickup coil and creating electrical resonance; the performance improvement degrades rapidly away from the resonant frequency; the capacitive shunt for the laminated- and the solid-based shunted device is better than that of the resistive shunt over a frequency bandwidth of 417 Hz and 576 Hz, respectively; controllers that can automatically tune the circuit's capacitance to track f_0 need to be developed in the future to expand the device's effective frequency bandwidth.
- Inductive load - the amount of stiffness variation $\bar{K}$ provided by the varying inductive load is the same as the resistive load; the stiffness K decreases monotonically as the load's impedance increases; tuning stiffness without appreciably affecting the system's damping is possible. Thus, this category of shunt would be used for vibration control strategies that only rely on stiffness tuning (e.g. adaptive vibration absorber, switched-stiffness vibration control, wave propagation control). Figure 6(b) shows that the Young's modulus variation is small once the inductance is beyond 200 mH. Therefore, an inductance less than 200 mH is needed for an actual device of this design. Nevertheless, varying the shunt inductance or capacitance with passive components can be a challenge. However, in some applications (e.g., switched-stiffness vibration control), only one inductor is needed along with a switch to connect and disconnect it to the device. Future work may focus on the implementation of existing active circuits that provide a synthetic electrical impedance to resolve the challenges in implementing a variable inductance.

By replacing the resistive load with energy storage units, this shunted device can scavenge useful electrical energy from the vibration. Hence, the stiffness and loss factor adaptation may not require an external power source. The power generation capability is summarized in table 3.

By comparing measurements from laminated Galfenol- and solid Galfenol-based shunted devices, the effect of eddy currents on shunted magnetostrictive devices has been studied and the key observations include:

- Stiffness tuning - the stress-induced eddy currents prevent magnetic moment rotation and decrease magnetostriction. Thus, eddy currents reduce $\bar{K}$ for each type of electrical shunt.
- Damping - stronger eddy currents increase the loss in the magnetostrictive element, but were found to reduce the total loss of the device due to a reduction in the magneto-electric coupling. As a result, devices containing laminated rods provide higher total damping capability than those containing solid rods.
- Energy harvesting - the eddy currents induce magnetic field diffusion, limit magnetic flux density variation, and reduce the electrical power produced by the shunted magnetostrictive device. Hence, eddy currents are detrimental to energy generation over the entire frequency range.

Lastly, this study considered a simplified vibration control device that is similar to the shunted magnetostrictive device without the coil or shunt circuit. This device is simpler and potentially more compact than the shunted magnetostrictive device and can be directly integrated into structures. This device can be adaptive via pre-load. It exhibits a loss factor ranging from 0.003 to 0.043 and $\bar{K}$ of 19.3% at 1 kHz as the bias compression changes from 604 N to 2364 N.

6. Concluding remarks

This study presents an experimental characterization of a shunted magnetostrictive device for vibration control applications. The device consists of a magnetostrictive rod (solid or laminated, <100>-oriented, highly-textured, polycrystalline $Fe_{81.6}Ga_{18.4}$), a coil, a permanent magnet array, a flux return path, and a shunt circuit. Because of the unique ΔE effect of magnetostrictive materials, the stiffness of this device can be continuously tuned in real-time by varying the shunt's electrical impedance. An inductive shunt can be used to create a moderate change in stiffness (up to 11%) without appreciably affecting the damping. By utilizing a variable shunt capacitance, the device can be used to create a variable mechanical notch filter.

This device can also attenuate unwanted structural vibrations due to its magneto-electric coupling and the magnetostrictive element's material hysteresis and eddy current loss. The loss factor of the system can also be tuned by varying the shunt's electrical impedance. Shunted magnetostrictive devices can provide moderate damping (loss factor > 0.06) over a relatively broad frequency range via resistive shunts and very high damping (loss factor > 1.3) over a narrow band via capacitive shunts.

Unlike most vibration damping solutions, this device is mechanically stiff and has no moving parts. Therefore, it can be designed to be an integral part of the structure. By attaching

the electric circuit to an energy harvesting and storage unit, this device can scavenge useful electricity from ambient vibrations. Therefore, the stiffness and damping tuning can potentially be self-powered.

6. Acknowledgment

We wish to acknowledge the member organizations of the Smart Vehicle Concepts Center, a National Science Foundation Industry-University Cooperative Research Center (www.SmartVehicleCenter.org) established under NSF Grant IIP-1738723. J.J.S. and V.M.A. would also like to acknowledge support from NASA's Revolutionary Vertical Lift Technology (RVLT) Project.

ORCID iDs

Zhangxian Deng https://orcid.org/0000-0003-1084-1738
Justin J Scheidler https://orcid.org/0000-0001-9696-1081
Marcelo J Dapino https://orcid.org/0000-0003-4888-1903

References

[1] Friswell M I and Flores E S 2013 Dynamic isolation systems using tunable nonlinear stiffness beams *Eur. Phys. J. Spe. Top.* **222** 1563–73
[2] Liu J and Liu K 2006 A tunable electromagnetic vibration absorber: Characterization and application *J. Sound Vib.* **295** 708–24
[3] Mcdaid A J and Mace B R 2013 A self-tuning electromagnetic vibration absorber with adaptive shunt electronics *Smart Mater. Struct.* **22** 105013
[4] Davis C L and Lesieutre G A 2000 An actively tuned solid-state vibration absorber using capacitive shunting of piezoelectric stiffness *J. Sound Vib.* **232** 601–17
[5] Scheidler J J and Asnani V M 2017 Validated linear dynamic model of electrically-shunted magnetostrictive transducers with application to structural vibration control *Smart Mater. Struct.* **26** 035057
[6] Asnani V M, Deng Z, Scheidler J J and Dapino M J 2015 Experimental comparison of piezoelectric and magnetostrictive shunt dampers in *Proc. of SPIE* Las Vegas, NV 98010R
[7] Clark A E and Savage H 1974 Giant magnetically induced changes of the elastic moduli in Tb.3Dy.7Fe2 Naval Ordnance Lab, White Oak, MD, USA
[8] Kellogg R and Flatau A B 2007 Experimental investigation of Terfenol-D's elastic modulus *J. Intell. Mater. Syst. Struct.* **19** 583–95
[9] Deng Z, Scheidler J J, Asnani V M and Dapino M J 2016 Quasi-static major and minor strain-stress loops in textured polycrystalline Fe81.6Ga18.4 Galfenol *J. Appl. Phys.* **120** 243901
[10] Datta S, Atulasimha J, Mudivarthi C and Flatau A 2010 Stress and magnetic field-dependent Young's modulus in single crystal iron–gallium alloys *J. Magn. Magn. Mater.* **322** 2135–44
[11] Teter J, Hathaway K and Clark A 1996 Zero field damping capacity in $(Tb_xDy_{1-x})Fe_y$ *J. Appl. Phys.* **79** 6213–15
[12] Wun-Fogle M, Restorff J B, Clark A E and Snodgrass J 2003 Magnetomechanical damping capacity of $Tb_xDy_{1-x}Fe_{1.92}(0.30 \leq x \leq 0.50)$ alloys *IEEE Trans. Magn.* **39** 3408–10
[13] Ho K K, Kerrigan C, Luna O and Carman G P 2005 Stoichiometric study of $Tb_{(x)}Dy_{(1-x)}Fe_2$ particulate composites for passive damping *Proc. of SPIE* San Diego, CA vol 5762 pp 245–52
[14] Hathaway K, Clark A and Teter J 1995 Magnetomechanical damping in giant magnetostriction alloys *Metall. Mater. Trans.* A **26** 2797–801
[15] Restorff J, Wun-Fogle M and Summers E 2011 Hysteresis, d^*_{33} and d_{33} of $Fe_{81.6}Ga_{18.4}$ textured polycrystals *J. Appl. Phys.* **109** 07A922
[16] Kerrigan C, Ho K, Mohanchandra K and Carman G 2008 Sputter deposition and analysis of thin film nitinol/terfenol-d multilaminate for vibration damping *Smart Mater. Struct.* **18** 015007
[17] Pulliam W J, Lee D, Carman G P and McKnight G P 2003 Thin-layer magnetostrictive composite films for turbomachinery fan blade damping *Proc. of SPIE* San Diego, CA vol 5054 pp 360–72
[18] Scheidler J J and Dapino M J 2016 Mechanically induced magnetic diffusion in cylindrical magnetoelastic materials *J. Magn. Magn. Mater.* **397** 233–9
[19] Deng Z and Dapino M J 2018 Dynamic model for magnetostrictive systems with applications to damper design *IEEE/ASME Trans. Mechatronics* **23** 1–11
[20] Scheidler J, Asnani V M and Dapino M J 2016 Dynamic characterization of Galfenol (Fe81.6Ga18.4) *NASA Technical Report* 2016–218754
[21] Scheidler J J, Asnani V M and Dapino M J 2016 Frequency-dependent, dynamic sensing properties of polycrystalline Galfenol (Fe81.6Ga18.4) *J. Appl. Phys.* **119** 244902
[22] Davino D, Giustiniani A, Visone C and Adly A 2011 Experimental analysis of vibrations damping due to magnetostrictive based energy harvesting *J. Appl. Phys.* **109** 07E509
[23] Yoo J, Murray A and Flatau A B 2014 Evaluation of magnetostrictive shunt damper performance using iron (Fe)-gallium (Ga) alloy in *Proc. of SPIE* San Diego, CA p 90573I
[24] Deng Z and Dapino M J 2017 Influence of electrical impedance and mechanical bistability on Galfenol-based unimorph harvesters *J. Intell. Mater. Syst. Struct.* **28** 421–31
[25] Deng Z 2015 Nonlinear modeling and characterization of the villari effect and model-guided development of magnetostrictive energy harvesters and dampers *PhD dissertation* Department of Mechancial Engineering, The Ohio State University
[26] Deng Z and Dapino M J 2017 Magnetic flux biasing of magnetostrictive sensors *Smart Mater. Struct.* **26** 055027
[27] Deng Z, Asnani V M and Dapino M 2015 Magnetostrictive vibration damper and energy harvester for rotating machinery *Proc. of Spie* San Diego, CA p 94330C
[28] ASTM Stardards D5992-96 2011 Standard guide for dynamic testing of vulcanized rubber and 618 rubber-like materials using vibratory methods (West Conshohocken, PA: ASTM International)
[29] Ungar E E and Kerwin E M 1962 Loss factors of viscoelastic systems in terms of energy concepts *J. Acoust. Soc. Am.* **34** 954–7
[30] Engdahl G 2000 *Magnetostrictive Materials Handbook* (San Diego: Academic)
[31] Deng Z 2017 Dynamic discrete energy-averaged model for magnetostrictive materials *J. Magn. Magn. Mater.* **441** 757–63
[32] Deng Z 2013 An energy-based dynamic loss hysteresis model for giant magnetostrictive materials *Int. J. Solids Struct.* **50** 672–9